ORIGINAL ARTICLE

Correlative analyses between tissue-based hypoxia biomarkers and hypoxia PET imaging in head and neck cancer patients during radiochemotherapy—results from a prospective trial

Nils H. Nicolay [1,2] · Nicole Wiedenmann [1,2] · Michael Mix [3] · Wolfgang A. Weber [4] · Martin Werner [2,5] · Anca L. Grosu [1,2] · Gian Kayser [2,5]

Abstract

Purpose Tumor hypoxia impairs the response of head-and-neck cancer (HNSCC) patients to radiotherapy and can be detected both by tissue biomarkers and PET imaging. However, the value of hypoxia biomarkers and imaging for predicting HNSCC patient outcomes are incompletely understood, and potential correlations between tissue and PET data remain to be elucidated. Here, we performed exploratory analyses of potential correlations between tissue-based hypoxia biomarkers and longitudinal hypoxia imaging in a prospective trial of HNSCC patients.

Methods Forty-nine patients undergoing chemoradiation for locally advanced HNSCCs were enrolled in this prospective trial. They underwent baseline biopsies and [^{18}F]FDG PET imaging and [^{18}F]FMISO PET at weeks 0, 2, and 5 during treatment. Immunohistochemical analyses for p16, Ki67, CD34, HIF1α, CAIX, Ku80, and CD44 were performed, and HPV status was assessed. Biomarker expression was correlated with biological imaging information and patient outcome data.

Results High HIF1α tumor levels significantly correlated with increased tumor hypoxia at week 2 as assessed by the difference in the [^{18}F]FMISO tumor-to-background ratios, and high HIF1α and CAIX expressions were both associated with a deferred decrease in hypoxia between weeks 2 and 5. Loco-regional recurrence rates after radiotherapy were significantly higher in patients with high CAIX expression and also increased for high levels of the DNA repair factor Ku80. HPV status did not correlate with any of the tested hypoxia biomarkers, and HPV-positive patients showed higher loco-regional control rates and progression-free survival independent of their hypoxia dynamics.

Conclusion In this exploratory trial, high expression of the tissue-based hypoxia biomarkers HIF1α and CAIX correlated with adverse hypoxia dynamics in HNSCCs during chemoradiation as assessed by PET imaging, and high CAIX levels were associated with increased loco-regional recurrence rates. Hence, hypoxia biomarkers warrant further investigations as potential predictors of hypoxia dynamics and hypoxia-associated radiation resistance.

✉ Nils H. Nicolay
   nils.nicolay@uniklinik-freiburg.de

1 Department of Radiation Oncology, Medical Center – University of Freiburg, Faculty of Medicine, University of Freiburg, Robert-Koch-Str. 3, 79106 Freiburg, Germany

2 German Cancer Consortium (DKTK), Partner Site Freiburg and German Cancer Research Center (DKFZ), Heidelberg, Germany

3 Department of Nuclear Medicine, Medical Center – University of Freiburg, Faculty of Medicine, University of Freiburg, Freiburg, Germany

4 Department of Nuclear Medicine, Technical University of Munich, Munich, Germany

5 Institute of Surgical Pathology, Department of Pathology, Medical Center – University of Freiburg, Faculty of Medicine, University of Freiburg, Freiburg, Germany

Introduction

Squamous cell head-and-neck cancers (HNSCC) are common malignancies, and almost one million patients are newly diagnosed with HNSCCs every year [1]. Radiation therapy, often combined with systemic treatment for advanced stages, is a primary treatment option for HNSCC patients, and several trials have demonstrated 5-year survival rates of about 50% [2, 3]. The response to radiotherapy seems to depend on biological tumor characteristics, and tumor-associated hypoxia is believed to be a major factor resulting in increased resistance of tumor cells to ionizing radiation [4]. Several means have been investigated to detect and monitor tumor-associated hypoxia in the context of radiation therapy, including tumor histology, tissue- and blood-based biomarkers and different imaging modalities [5–7]. The relevance of hypoxia dynamics in HNSCC patients for the prediction of radiotherapy response has been unclear, and potential roles of individual hypoxia surrogate markers have remained somewhat controversial [8, 9].

Fluorine-18 misonidazole ($[^{18}F]$FMISO) tracer uptake has been widely demonstrated to correlate well with tissue oxygen measurements, and positron emission tomography (PET) using $[^{18}F]$FMISO has been established as a reliable means for the noninvasive detection of hypoxic areas within tissues [10, 11]. The role of $[^{18}F]$FMISO imaging for the prediction of radiation response has been subject to several clinical trials [12–14]. However, the value of hypoxia PET imaging for predicting the radiation response of HNSCC remains incompletely understood, and the correlation of PET-derived hypoxia information with molecular tumor characteristics relevant for hypoxia signaling and the response to ionizing radiation is still the focus of research.

The aim of this exploratory analysis was to investigate if the expression of certain tissue markers prior to treatment could be used as a predictor for the development or resolution of hypoxia during the course of chemoradiation and may therefore be used to stratify or adjust radiation treatment. While tumor biopsies are commonly available for HNSCC patients undergoing definitive chemoradiation and can be easily analyzed for hypoxia markers, longitudinal $[^{18}F]$FMISO PET/CT during treatment is time-consuming and requires strong additional efforts and resources.

We set up a prospective clinical trial investigating the feasibility and potential predictive value of hypoxia surveillance in HNSCC patients. All enrolled patients received in-depth histopathological investigations including tissue-based hypoxia analyses at baseline and underwent $[^{18}F]$FMISO PET/CT scans before the initiation of treatment and in weeks 2 and 5 during chemoradiation. Molecular markers associated with tumor hypoxia and radiation response were correlated with clinical outcome and hypoxia dynamics derived from $[^{18}F]$FMISO imaging.

Patients and methods

Patients and treatment

Forty-nine patients with locally advanced HNSCC were enrolled in this prospective monocentric trial (16 patients in the pilot trial, 33 additional patients in the main trial). While all patients in the pilot and main trial received pre-treatment biopsies and PET imaging to the same specifications, patients in the main trial also received repeat multiparametric MRI examinations during treatment that will be reported elsewhere. Patients were predominantly male ($n = 44$; 89.8%) with a median age of 60 years (34 to 78 years). Tumors were mostly

Table 1 Patient characteristics

Patient characteristics	n	%
Age (years)		
Median	60	
Minimum	34	
Maximum	78	
Gender		
Male	44	89.8
Female	5	10.2
Tumor location		
Oral cavity	2	4.1
Oropharynx	19	38.8
Hypopharynx	12	24.5
Larynx	7	14.3
Multi-level	9	18.4
Tumor extent		
T1	1	2.0
T2	4	8.2
T3	14	28.6
T4	30	61.2
Nodal status		
N0	4	8.2
N1	1	2.0
N2a	0	0.0
N2b	9	18.4
N2c	35	71.4
HPV status		
HPV positive	9	18.4
HPV negative	40	81.6

staged as T3 ($n = 14$; 28.6%) or T4 ($n = 30$; 61.2%), and nodal disease was present in 45 patients (91.8%), of whom 35 had contralateral or bilateral lymphatic spread (71.4%). Patient characteristics are listed in Table 1. All patients were treated with definitive chemoradiation; image-guided intensity-modulated radiotherapy was applied to a cumulative dose of 70 Gy in fractions of 2 Gy over 7 weeks; additionally, patients received systemic treatment with up to 3 cycles of cisplatin (100 mg/m^2 body surface area in weeks 1, 4, and 7). Locoregional control (LRC), progression-free survival (PFS), distant metastasis-free survival (DFS), and overall survival (OS) were measured from the initiation of treatment. Written informed consent was provided by all patients prior to enrolment. The trial and the imaging and biomarker analyses were approved by the Independent Ethics Committee of the University of Freiburg (reference no. 479/12) and were carried out in accordance with the Declaration of Helsinki (revised version of 2008). The trial was registered with the German Clinical Trial Register (DRKS00003830).Imaging

All patients received a planning computed tomography (CT) and magnetic resonance imaging (MRI) scan as part of the radiotherapy planning procedures as well as PET imaging with 18F-fluorodeoxyglucose ([18F]FDG) and [18F]FMISO tracers prior to treatment. Additional [18F]FMISO PET/CT scans were performed in weeks 2 and 5 during chemoradiation. PET imaging for the first 15 patients was performed on an ECAT EXACT 921 PET scanner (Siemens, Erlangen, Germany) and for the consecutive 34 patients on a Gemini TrueFlight PET/CT scanner (Philips, Hamburg, Germany). The administered [18F]FMISO activity was 3.7 MBq/kg to a maximum activity of 370 MBq; hypoxia imaging was carried out at 150 min after [18F]FMISO administration (3 frames at 10 min each, followed by a transmission scan for 5 min). PET imaging was carried out in radiation treatment position using a thermoplastic head immobilization mask, and all PET images were co-registered to the corresponding planning CTs using a mutual information algorithm. Quantitative analyses were performed using a sum of three attenuation-corrected frames [15]. The primary endpoint of this trial was a quantitative assessment of the [18F]FMISO dynamics during HNSCC chemoradiation.

The gross tumor volumes (GTVs) were manually delineated on [18F]FDG-PET-MRI co-registered images with the tumor volumes being determined by a 40% threshold of the maximum SUV obtained within the tumor [15]. GTVs were individually cross-validated with the co-registered planning CT scans by 2 experienced physicians. Hypoxic subvolumes were defined as all voxels within the GTV that demonstrated a ratio of [18F]FMISO SUV to mean SUV in the contralateral sternocleidomastoideus muscles exceeding 1.4. This ratio was based on published thresholds and has previously been successfully validated in this patient cohort [15, 16].

The imaging parameters used for this correlative analysis were the baseline tumor volumes according to the GTV delineation (in milliliters), the hypoxic subvolumes based on the [18F]FMISO uptake ratio (in milliliters), and the ratio of maximum SUV in the tumor to the mean SUV in the muscles at baseline and during weeks 2 and 5 (normalized [18F]FMISO SUVmax). The dynamics of tumor-associated hypoxia during treatment were assessed by subtracting the normalized [18F]FMISO SUVmax at baseline from the SUVmax values at week 2 or week 5 and quantifying the percentage of change.

Immunohistochemistry

All patients received tumor biopsies prior to treatment initiation to confirm diagnosis. Tumor samples were formalin-fixed and paraffin-embedded according to routine histopathology protocols. After sectioning at 2 μm, tumor slices were mounted on coated glass slides (Langenbrinck, Emmendingen, Germany), deparaffinized and rehydrated through descending graded concentrations of ethanol. Heat-induced antigen retrieval was carried out and endogenous peroxidase activity was inhibited by incubation with H_2O_2 for 5 min. Mouse linker (DAKO) and Envison Flex Kit using horseradish peroxidase-diaminobenzidine (HRP-DAB) reaction (DAKO) as chromogen were applied for antigen-complex visualization. Primary antibody specification and antigen retrieval are listed in supplementary table 1. All slides were counterstained by hematoxylin.

Tissue specimens were assessed for hypoxia markers hypoxia-inducible factor 1α (HIF1α), carbonic anhydrase 9 (CAIX), and the endothelial marker CD34. HIF1α acts as a transcription factor and is considered the master transcriptional regulator influencing cellular responses to tissue hypoxia [17]. The transmembrane metalloenzyme CAIX is commonly overexpressed in hypoxic solid tumors and participates in tumor acidification and extracellular hypoxia-driven acidosis [18]. CD34 is a phosphoglycoprotein expressed in endothelial cells and has been suggested as a marker for tumor microvascular density and hence as an indirect hypoxia marker in HNSCC [19]. Antigen Ki67 was assessed as a marker of cellular proliferation, and CD44 as a marker for HNSCC-associated cancer stem cells, as both the HNSCCs' proliferative activity and cancer stem cell development have been linked to tumor hypoxia [20, 21]. Additionally, the non-homologous end joining DNA repair factor Ku80 was quantified as increasing evidence suggests an interplay between tumor hypoxia, treatment resistance, and enhanced DNA double-strand break repair [22].

For HIF1α, CAIX, CD44, and Ku80, slides were assessed in a semi-quantitative manner using the H-score. Staining intensity (0 = no staining, 1 = weak, 2 = moderate, 3 = strong) was assessed in all viable tumor cells. The sum of the tumor cell percentages of the different staining intensities multiplied by their specific intensity score resulted in the H-score (range 0–300). Microvessel density assessed by CD34 staining was divided into three categories: 1, only larger vessels in the stroma, no contact to

tumor cells; 2, smaller vessels in the stroma with contact to tumor cells, no vessels intermingled in the tumor-stroma border; 3, small vessels intermingling with tumor cells at the tumor-stroma border. For Ki67 stainings, all tumor cells were evaluated for positivity, and percentage with regard to all viable tumor cells was calculated.

P16 overexpression was considered if more than 70% of viable tumor cells showed strong nuclear and/or cytoplasmic staining.

HPV analyses

Tumor microdissections were carried out from tumor tissue in the biopsies, and DNA was extracted according to routine clinical protocols. HPV-specific DNA was detected using a HPV 3.5 LCD array (Chipron, Berlin, Germany) according to the manufacturer's instructions, and results were provided as a binary score.

Statistical analyses

Statistical analyses were performed to investigate potential correlations between individual tumor tissue variables and between tumor tissue variables and imaging variables as outlined above. Statistical significance of pairs of variables was tested using Pearson's product-moment correlation. Clinical outcome parameters were analyzed using the Kaplan-Meier method, and correlations between individual tumor tissue variables and clinical outcome parameters were tested for statistical significance using the logrank test and the Cox proportional hazards model. For all statistical analyses, $p < 0.05$ was considered statistically significant. As this was an exploratory analysis to generate hypotheses regarding potential correlations that need verification in a confirmatory analysis, no adjustment for multiple testing was performed.

Results

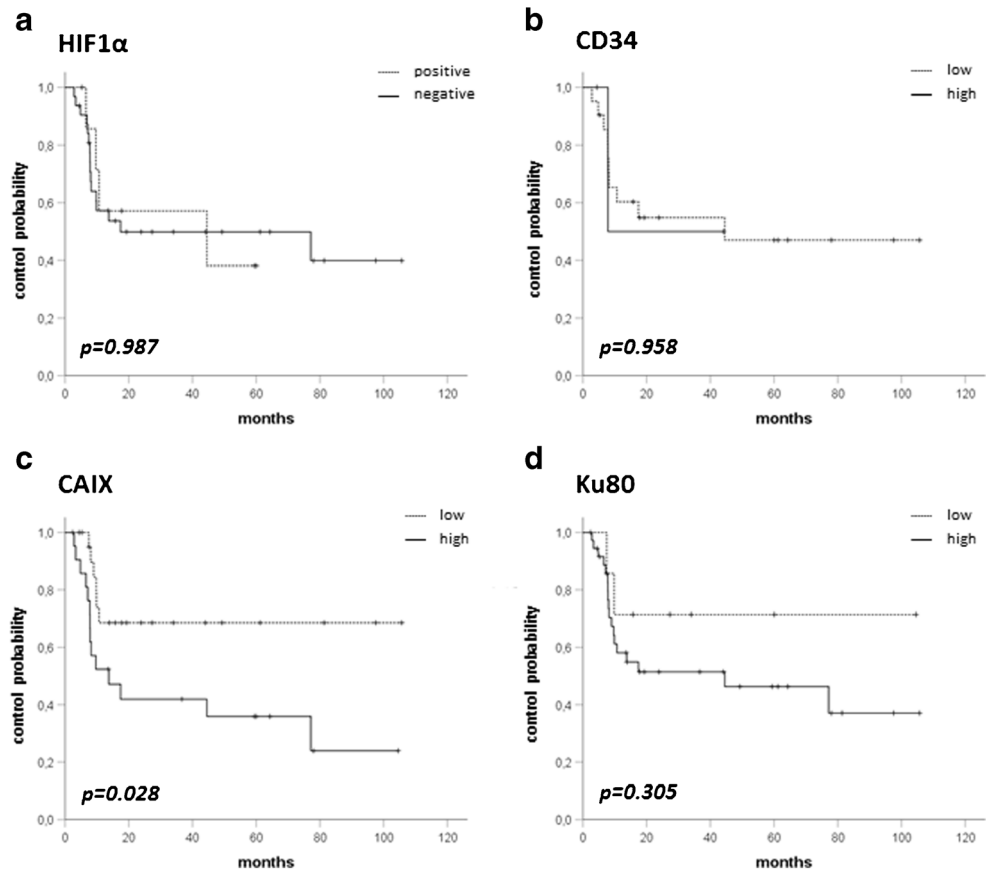### Correlative analyses between tissue biomarkers and clinical outcome parameters

Forty-nine patients were included in this trial, and sufficient biological material for analysis of all tissue markers was available from tumor biopsies of 44 patients, while due to the small biopsy sizes, only some biomarker analyses could be carried out for the remaining 5 patients. HPV status was assessed by HPV DNA and p16 expression analyses, and tumor grade, Ki67 and CD44 were quantified as markers for tumor proliferation and cancer stem cell content, respectively. Additionally, the density of the CD34-positive microvasculature and the H-scores for hypoxia-inducible factor 1α (HIF1α) and carbonic anhydrase 9 (CAIX) were measured as potential surrogate tissue markers for tumor hypoxia, and Ku80 expression was

investigated as a repair marker for radiation-induced DNA damage. LRC, OS, PFS, and DFS were determined for each patient and correlated with the individual tissue biomarkers. In our analysis, only HPV status and CAIX expression were found to correlate with LRC: In accordance with previous reports, patients with HPV-positive tumors demonstrated significantly improved LRC (hazard ratio 0.133 [0.018–0.988]; $p = 0.049$) and PFS (hazard ratio 0.232 [0.055–0.983]; $p = 0.047$) and a trend towards improved OS (hazard ratio 0.03 [0.001–1.731]; $p = 0.090$) and DFS (hazard ratio 0.198 [0.024–1.609]; $p = 0.130$), serving as an internal validation for the biomarker analysis (supplementary figure 1A and 2) [23]. p16 expression correlated non-significantly with improved LRC (hazard ratio 0.230 [0.030–1.739]; $p = 0.155$) (supplementary figure 1B). Patients with high H-scores for CAIX expression demonstrated significantly reduced LRC rates (hazard ratio 2.803 [1.075–7.309]; $p = 0.035$), while the other hypoxia markers HIF1α and CD34-positive microvascular density did not correlate with clinical outcome (Fig. 1a–c). No other tissue markers were found to relate to clinical endpoints, although high Ku80 H-scores demonstrated a trend towards reduced LRC (hazard ratio 2.112 [0.490–9.110]; $p = 0.316$) with the Kaplan-Meier curves separating after the first year of follow-up (Fig. 1d and supplementary figure 3). High levels of both CAIX and Ku80 in tumor specimens demonstrated a strong correlation with decreased LRC (hazard ratio 3.831 [1.469–9.990]; $p = 0.006$) and PFS (hazard ratio 2.397 [1.036–5.547]; $p = 0.041$) (Fig. 2a, b).

Correlative analyses between tissue biomarkers and hypoxia PET imaging

Expression levels of tissue biomarkers were correlated with the obtained PET/CT information using Pearson's correlation coefficient. Initial tumor volumes as assessed by pre-treatment MRI/[^{18}F]FDG-PET/CT imaging varied between 1.10 and 212.25 ml (median 38.16 ml), and hypoxic subvolumes in the primary tumor measured by [^{18}F]FMISO PET/CT ranged between 0 and 73.90 ml (median 14.54 ml) (Fig. 3, supplementary figure 4). High H-scores of the hypoxia marker HIF1α in the tumor were found to significantly correlate with an increase in tumor hypoxia during the first 2 weeks of treatment as assessed by the difference in the tumor-to-background ratios between baseline and week 2 ($r = 0.346$; $p = 0.034$) (Fig. 4a). Additionally, high expression of hypoxia biomarkers HIF1α and CAIX were both related to a deferred decrease in [^{18}F]FMISO uptake between weeks 2 and 5 ($r = -0.330$, $p = 0.049$ for HIF1α; $r = -0.416$, $p = 0.011$ for CAIX) (Fig. 4b, supplementary figure 5). No correlations were found between baseline [^{18}F]FMISO hypoxia signals and HIF1α or CAIX expression, and no other tissue markers correlated with [^{18}F]FMISO-based hypoxic tumor volumes or hypoxia dynamics in our patient cohort. High H-scores of the cancer stem cell marker CD44 inversely correlated with larger

Fig. 1 High CAIX expression correlates with worse loco-regional control in HNSCC patients. **a** LRC rates for HIF1α-positive and HIF1α-negative HNSCCs. **b** LRC rates for low and high CD34-positive micro-vascular density. **c** LRC rates for low and high expression of CAIX. **d** LRC rates for low and high expression of the DNA repair marker Ku80. p values are derived from logrank test

tumor volumes at baseline ($r = -0.376$; $p = 0.013$). Details are listed in supplementary table 2.

Correlative analyses between individual tissue biomarkers

Pairwise correlations between expression levels of individual tissue biomarkers were performed using Pearson's correlation coefficient. As expected, HPV DNA in tumor tissue strongly correlated with p16 expression ($r = 0.801$; $p = 0.001$). Detection of p16 was found inversely correlated with high

levels of for the cancer stem cell marker CD44 ($r = -0.328$; $p = 0.047$). No significant correlations were found within the analyzed tissue-based hypoxia markers, and no correlations could be detected for any of the other biomarkers. Statistical details are outlined in Table 2.

Discussion

The potential of tumor-specific biological or functional information to predict the response to radiation therapy could form

Fig. 2 High expression of both CAIX and Ku80 in HNSCCs predicts decreased loco-regional control and progression-free survival. **a** LRC rates for tumors with a high expression of both CAIX and Ku80. **b** PFS rates for tumors with a high expression of both CAIX and Ku80. p values are derived from logrank test
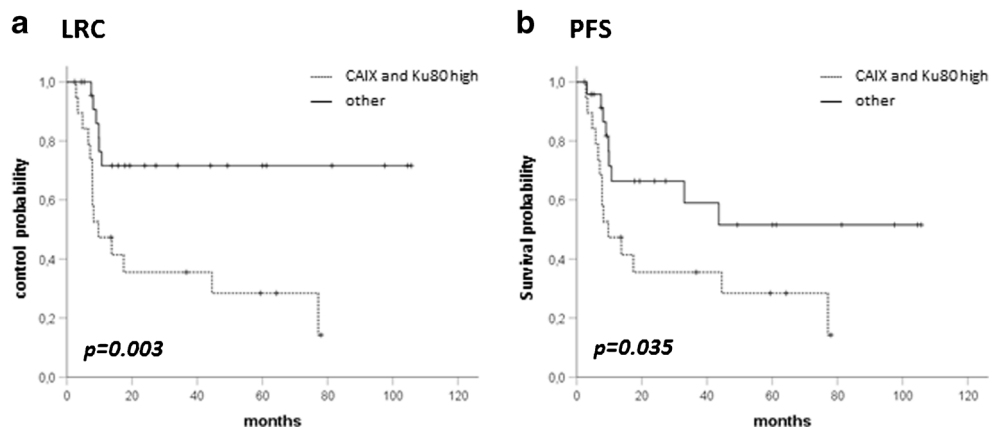
Fig. 3 Representative images demonstrating the differential dynamics of tumor and hypoxic subvolumes during the course of chemoradiation. **a** Time course of tumor volumes (red contours) and hypoxic tumor subvolumes (purple contours) from week 0 to 5 for a representative patient with early (week 0 to 2) resolution of tumor hypoxia. **b** Time course of tumor and hypoxic subvolumes for a representative patient with delayed (week 2 to 5) resolution of tumor hypoxia
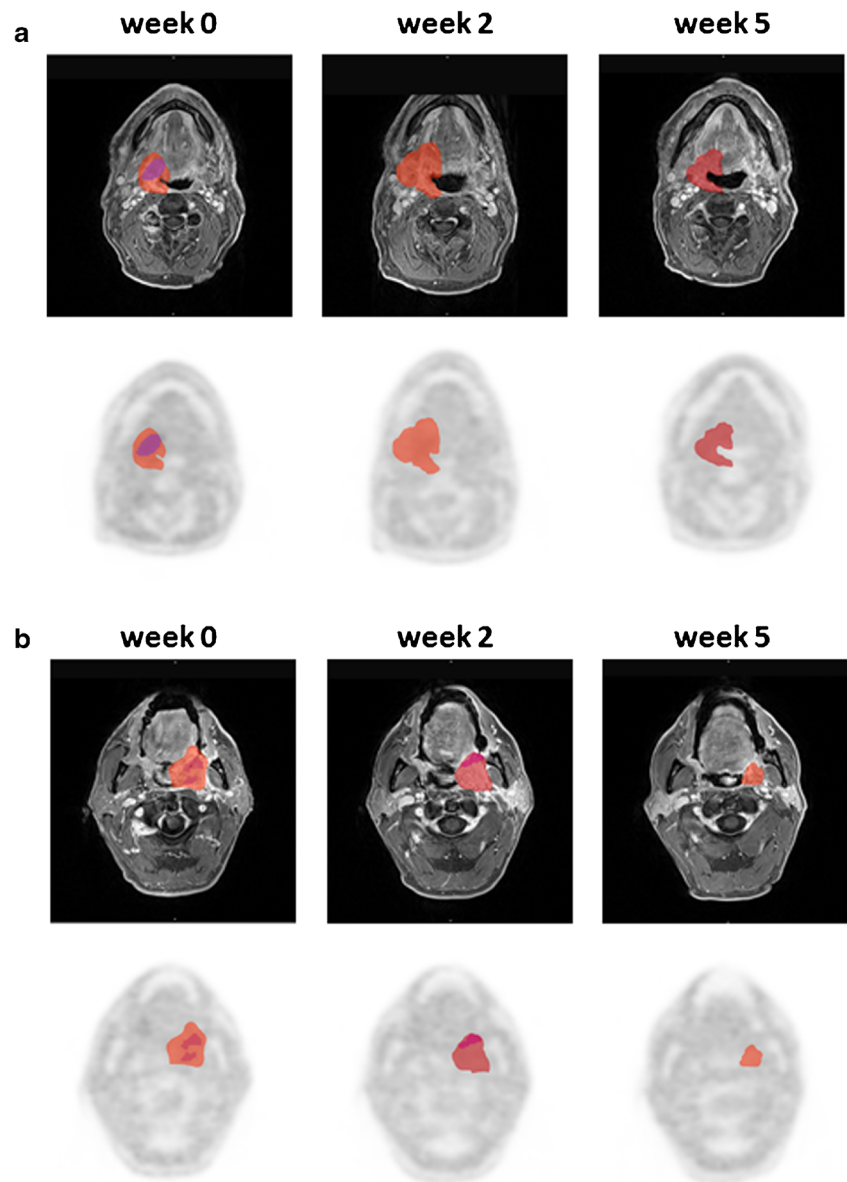
the basis for the development of personalized radiation treatment planning and monitoring. While functional imaging modalities can be used to non-invasively and longitudinally monitor tumor characteristics and response patterns over the course of a treatment, evidence for clear correlations with the underlying tumor biology remains scarce. In HNSCCs, tumor hypoxia has been shown to increase resistance to ionizing radiation, and [18F]FMISO PET imaging has been proposed as a valuable means of tracing and monitoring hypoxia during radiation therapy [10]. Previous publications have demonstrated better loco-regional control rates for tumors with low initial hypoxia as assessed by [18F]FMISO uptake or a disappearance of residual PET-detected hypoxia during the first weeks of radiotherapy [12, 15, 24].

Here, we analyzed potential connections between [18F]FMISO PET imaging and tissue-based biological markers for tumor hypoxia in a prospective trial of HNSCC patients undergoing chemoradiation. Intratumoral density of CD34-positive microvessels and the expression levels of the hypoxia-inducible transcription factor HIF1α and the membrane-bound enzyme CAIX were chosen as tissue-based surrogate markers for hypoxia. HIF1α has been proposed as the transcriptional master regulator for the cellular responses to hypoxic conditions, and previous analyses have demonstrated an influence of HIF1α on various processes influencing cellular radiation resistance, including DNA repair and maintenance of cancer stem cells [21, 22, 25]. CAIX is strongly induced by HIF1α and participates in tissue acidification during hypoxic conditions, while the endothelial marker CD34 reflects the density of microvessels and indirectly mirrors tumor hypoxia [18, 19]. While all three factors have been clearly linked to tumor hypoxia in animal models, to our
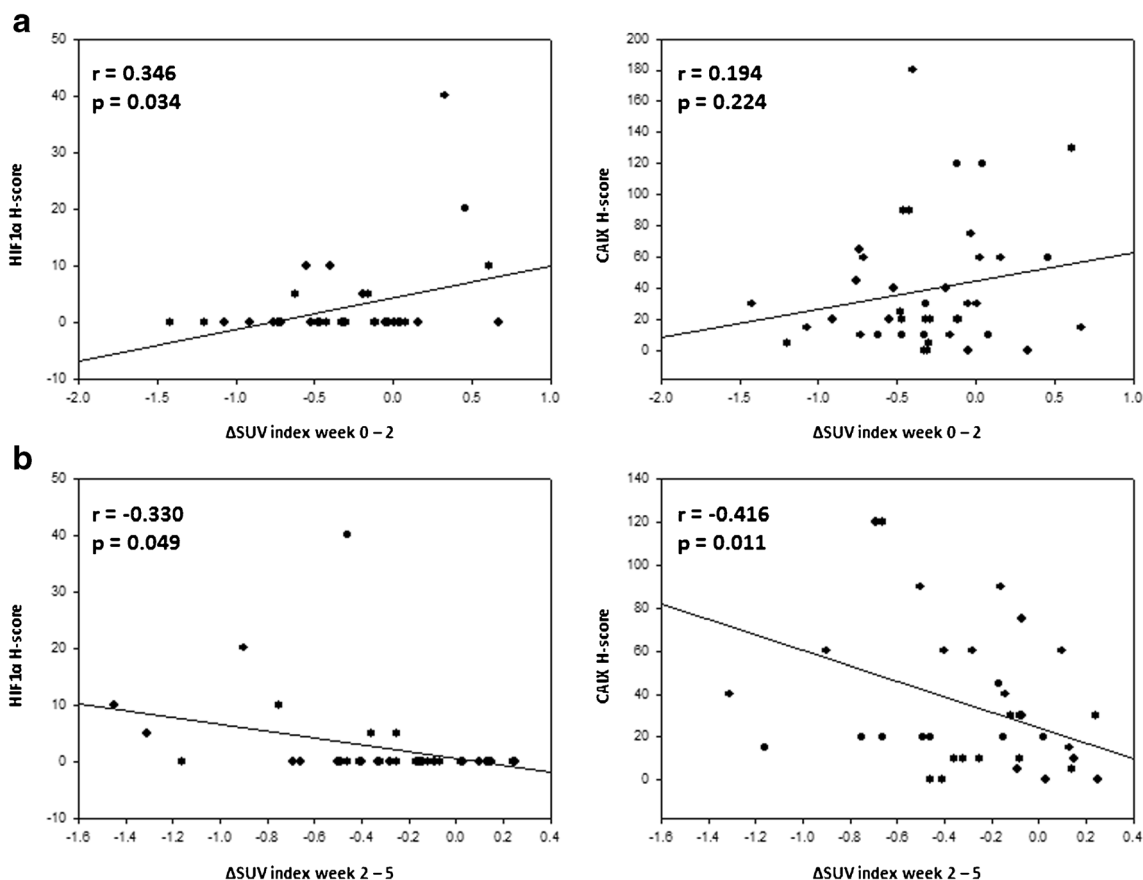
Fig. 4 High expression of hypoxia markers correlates with delayed resolution of the [^{18}F]FMISO hypoxia signal. **a** Correlations between H-scores of HIF1α and CAIX and increases in [^{18}F]FMISO ΔSUV index between weeks 0 and 2. **b** Correlations between H-scores of HIF1α and CAIX and delayed decreases in [^{18}F]FMISO ΔSUV index between weeks 2 and 5

knowledge, no analyses are available that investigated correlations between these tissue-based hypoxia biomarkers and

dynamic hypoxia imaging in HNSCC patients [26]. In our analysis, HIF1α expression correlated with an increase in

Table 2 Pairwise correlations between individual biomarkers. R and p values are derived from Pearson correlation coefficient. *$p < 0.05$

		Ki67	CD44	HPV	p16	HIF1α	CAIX	CD34	Ku80
Grade	r	−0.049	0.013	0.015	0.060	−0.093	−0.001	−0.051	0.132
	p	0.767	0.934	0.917	0.724	0.573	0.995	0.760	0.392
Ki67	r		−0.286	0.281	0.276	0.156	−0.143	0.184	−0.198
	p		0.077	0.083	0.098	0.343	0.386	0.263	0.226
CD44	r			−0.191	−0.328*	−0.019	0.065	0.126	0.103
	p			0.213	0.047	0.910	0.675	0.445	0.506
HPV	r				0.801*	−0.108	−0.159	−0.138	−0.189
	p				0.001	0.512	0.302	0.403	0.219
p16	r					−0.118	−0.237	−0.047	−0.179
	p					0.488	0.159	0.784	0.289
HIF1α	r						0.065	−0.146	0.052
	p						0.696	0.374	0.752
CAIX	r							−0.091	0.252
	p							0.580	0.099
CD34	r								−0.096
	p								0.562

Italicized entries are statistically significant values

intratumoral [^{18}F]FMISO uptake during the first 2 weeks of chemoradiation, and high levels of both HIF1α and CAIX were linked to a delayed resolution of the [^{18}F]FMISO signal between weeks 2 and 5. These [^{18}F]FMISO dynamics have previously been linked to decreased patient outcomes [12, 24]. In line with these findings, high CAIX signals translated into worse LRC rates after treatment in our patient cohort.

Several publications have analyzed the role of HIF1α and CAIX as prognostic and predictive biomarkers for HNSCC patients. The role of HIF1α in promoting radiation resistance has been widely studied in preclinical models and clinically, and it has been suggested that the hypoxia-mediated expression of HIF1α results in an efficient response to radiation-induced DNA damage and the evasion of apoptosis [27, 28]. HIF1α expression has been widely linked to reduced LRC and PFS in HNSCC patients undergoing radiotherapy, although absent or inverse correlations have also been reported [29–31]. Two previous studies have demonstrated a weak correlation between baseline [^{18}F]FMISO uptake and HIF1α expression in oral cavity cancers [32, 33]. HIF1α expression was found to correlate to pre-treatment [^{18}F]FMISO SUV$_{max}$ and tumor-to-background ratio [33]. However, both patient cohorts underwent surgical tumor excision, making the whole tumor tissue available for analyses, and HIF1α quantification was carried out in tissue regions pre-selected for their staining patterns. In our cohort, only tumor biopsies were available for hypoxia analyses as all patients underwent definitive chemoradiation, so no account could be made for the known intratumoral heterogeneity regarding hypoxic subvolumes [34].

Similarly, it has been suggested that CAIX expression relates to a reduced disease-specific survival [35–37]. Additionally, loco-regional response rates to radiation and chemoradiation therapies were found to correspond to high levels of CAIX within the tumor [6, 19, 38], and this effect has been attributed to an increased resistance to radiotherapy and chemotherapy [6, 39, 40]. So far, no clear link has been reported between CAIX expression and imaging-based or functional hypoxia analyses. In a previous report, CAIX failed to correspond with MRI-based tumor perfusion levels or baseline tumor pO$_2$ as surrogate markers for hypoxia [41, 42]. Nevertheless, HIF1α and CAIX expression corresponded to a distinct [^{18}F]FMISO dynamic and a delayed resolution of tumor hypoxia in our dataset, potentially predicting a decreased response to radiotherapy. This delayed hypoxia resolution and residual [^{18}F]FMISO uptake at week 2 has been suggested as the best prognosticator of LRC following chemoradiation [5, 12]. Initial increases in the [^{18}F]FMISO signal between weeks 0 and 2 during chemoradiation have been observed in previous studies, and it has been proposed that profound perfusion-limited hypoxia in the affected tumor areas may have hampered the initial [^{18}F]FMISO uptake and wash-out. Therefore, the [^{18}F]FMISO bound in these regions

may not correctly show the underlying hypoxia level [5]. HIF1α has been shown to induce vascular endothelial growth factor-mediated vascular normalization and reperfusion during radiotherapy and may thereby allow increased [^{18}F]FMISO uptake of severely hypoxic tumors at week 2 of chemoradiation [43, 44]. Therefore, on a mechanistic level, the observed correlation between high HIF1α and HIF1α-dependent CAIX expression with these distinct [^{18}F]FMISO dynamics may reflect the vascular effects of high HIF1α levels.

Efficient repair of radiation-induced DNA double-strand breaks has been suggested as a mechanism by which cells and tissues increase their resistance to ionizing radiation, and the non-homologous end joining repair proteins Ku70 and Ku80 have been linked to treatment failure after radiotherapy [45–47]. There is increasing evidence that the radiation resistance observed in hypoxic tumors is at least in part due to alterations in cellular DNA double-strand break repair, and there is an increasing understanding about the interplay between hypoxia and DNA damage recognition and repair signaling [22]. Hypoxia results in a shift from the high-fidelity homology-directed to the more error-prone repair through end joining, and HIF1α has been shown to influence the expression of key proteins involved in non-homologous end joining, including the DNA-dependent protein kinase as well as Ku70 and Ku80 [48, 49]. In our dataset, high Ku80 expression demonstrated a trend towards decreased LRC, and patients exhibiting high intratumoral levels of both CAIX and Ku80 exhibited a significant deterioration of LRC and PFS rates, suggesting that a combination of surrogate tissue markers for both tumor hypoxia and hypoxia-mediated DNA repair capacity may serve as a strong predictor of radiation response in HNSCC patients.

Despite bringing together a comprehensive imaging and biomarker dataset from a prospective trial, this exploratory analysis is limited by the rather small patient cohort, and this relatively small sample size somewhat limits the statistical possibilities of our analysis. Therefore, larger confirmatory analyses employing hypoxia imaging may be needed to corroborate our findings and to add statistical power, e.g., for detecting more complex tissue signatures that may be better suited to predict [^{18}F]FMISO dynamics and response to radiotherapy in HNSCC patients. Additionally, HNSCC tissue is well known for its heterogeneity regarding areas of varying hypoxia, and histology based on small biopsy samples cannot represent the whole tumor. The limited availability of cancer tissue may somewhat hamper further and more complex correlative analyses in this cohort of non-surgically treated patients.

In summary, we demonstrated that HIF1α and CAIX expression correlated with a delayed resolution of the [^{18}F]FMISO-based hypoxia signal in HNSCC patients, and high CAIX levels were able to predict loco-regional failure

after chemoradiation treatment, especially in patients also expressing the DNA repair marker Ku80. Validation in an independent confirmatory cohort will help to further clarify if baseline tissue-based hypoxia markers that are derived from routinely available biopsies can be used as potential surrogates for hypoxia dynamics in HNSCC patients.

Compliance with ethical standards

Conflict of interest The authors declare that they have no conflict of interest.

Ethical approval All procedures performed in studies involving human participants were in accordance with the ethical standards of the institutional and/or national research committee (Independent Ethics Committee of the University of Freiburg, reference no. 479/12) and with the 1964 Helsinki declaration and its later amendments or comparable ethical standards.

References

1. Bray F, Ferlay J, Soerjomataram I, Siegel RL, Torre LA, Jemal A. Global cancer statistics 2018: GLOBOCAN estimates of incidence and mortality worldwide for 36 cancers in 185 countries. *CA Cancer J Clin*. 2018;68(6):394–424.

2. Bonner JA, Harari PM, Giralt J, Azarnia N, Shin DM, Cohen RB, et al. Radiotherapy plus cetuximab for squamous-cell carcinoma of the head and neck. *N Engl J Med*. 2006;354(6):567–78.

3. Blanchard P, Baujat B, Holostenco V, Bourredjem A, Baey C, Bourhis J. Pignon JP, group M-CC: Meta-analysis of chemotherapy in head and neck cancer (MACH-NC): a comprehensive analysis by tumour site. *Radiother Oncol*. 2011;100(1):33–40.

4. Baumann R, Depping R, Delaperriere M, Dunst J. Targeting hypoxia to overcome radiation resistance in head & neck cancers: real challenge or clinical fairytale? *Expert Rev Anticancer Ther*. 2016;16(7):751–8.

5. Zips D, Zophel K, Abolmaali N, Perrin R, Abramyuk A, Haase R, et al. Exploratory prospective trial of hypoxia-specific PET imaging during radiochemotherapy in patients with locally advanced head-and-neck cancer. *Radiother Oncol*. 2012;105(1):21–8.

6. Kwon OJ, Park JJ, Ko GH, Seo JH, Jeong BK, Kang KM, et al. HIF-1alpha and CA-IX as predictors of locoregional control for determining the optimal treatment modality for early-stage laryngeal carcinoma. *Head Neck*. 2015;37(4):505–10.

7. Wiedenmann N, Bunea H, Rischke HC, Bunea A, Majerus L, Bielak L, et al. Effect of radiochemotherapy on T2* MRI in HNSCC and its relation to FMISO PET derived hypoxia and FDG PET. *Radiat Oncol*. 2018;13(1):159.

8. Eriksen JG, Overgaard J, Danish H. Neck Cancer Study G: Lack of prognostic and predictive value of CA IX in radiotherapy of squamous cell carcinoma of the head and neck with known modifiable hypoxia: an evaluation of the DAHANCA 5 study. *Radiother Oncol*. 2007;83(3):383–8.

9. Toustrup K, Sorensen BS, Nordsmark M, Busk M, Wiuf C, Alsner J, et al. Development of a hypoxia gene expression classifier with predictive impact for hypoxic modification of radiotherapy in head and neck cancer. *Cancer Res*. 2011;**71**(17):5923–31.

10. Rajendran JG, Schwartz DL, O'Sullivan J, Peterson LM, Ng P, Scharnhorst J, et al. Tumor hypoxia imaging with [F-18] fluoromisonidazole positron emission tomography in head and neck cancer. *Clin Cancer Res*. 2006;12(18):5435–41.

11. Rasey JS, Koh WJ, Evans ML, Peterson LM, Lewellen TK, Graham MM, et al. Quantifying regional hypoxia in human tumors with positron emission tomography of [18F]fluoromisonidazole: a pretherapy study of 37 patients. *Int J Radiat Oncol Biol Phys*. 1996;36(2):417–28.

12. Lock S, Perrin R, Seidlitz A, Bandurska-Luque A, Zschaeck S, Zophel K, et al. Residual tumour hypoxia in head-and-neck cancer patients undergoing primary radiochemotherapy, final results of a prospective trial on repeat FMISO-PET imaging. *Radiother Oncol*. 2017;124(3):533–40.

13. Sachpekidis C, Thieke C, Askoxylakis V, Nicolay NH, Huber PE, Thomas M, et al. Combined use of (18)F-FDG and (18)F-FMISO in unresectable non-small cell lung cancer patients planned for radiotherapy: a dynamic PET/CT study. *Am J Nucl Med Mol Imaging*. 2015;5(2):127–42.

14. Grkovski M, Lee NY, Schoder H, Carlin SD, Beattie BJ, Riaz N, et al. Monitoring early response to chemoradiotherapy with (18)F-FMISO dynamic PET in head and neck cancer. *Eur J Nucl Med Mol Imaging*. 2017;44(10):1682–91.

15. Wiedenmann NE, Bucher S, Hentschel M, Mix M, Vach W, Bittner MI, et al. Serial [18F]-fluoromisonidazole PET during radiochemotherapy for locally advanced head and neck cancer and its correlation with outcome. *Radiother Oncol*. 2015;117(1):113–7.

16. Bittner MI, Wiedenmann N, Bucher S, Hentschel M, Mix M, Weber WA, et al. Exploratory geographical analysis of hypoxic subvolumes using 18F-MISO-PET imaging in patients with head and neck cancer in the course of primary chemoradiotherapy. *Radiother Oncol*. 2013;108(3):511–6.

17. Calzada MJ, del Peso L. Hypoxia-inducible factors and cancer. *Clin Transl Oncol*. 2007;9(5):278–89.

18. Hilvo M, Baranauskiene L, Salzano AM, Scaloni A, Matulis D, Innocenti A, et al. Biochemical characterization of CA IX, one of the most active carbonic anhydrase isozymes. *J Biol Chem*. 2008;283(41):27799–809.

19. Ou D, Garberis I, Adam J, Blanchard P, Nguyen F, Levy A, et al. Prognostic value of tissue necrosis, hypoxia-related markers and correlation with HPV status in head and neck cancer patients treated with bio- or chemo-radiotherapy. *Radiother Oncol*. 2018;126(1):116–24.

20. Rodrigues M, Xavier FCA, Andrade NP, Lopes C, Miguita Luiz L, Sedassari BT, et al. Prognostic implications of CD44, NANOG, OCT4, and BMI1 expression in tongue squamous cell carcinoma. *Head Neck*. 2018;40(8):1759–73.

21. Schoning JP, Monteiro M, Gu W. Drug resistance and cancer stem cells: the shared but distinct roles of hypoxia-inducible factors HIF1alpha and HIF2alpha. *Clin Exp Pharmacol Physiol*. 2017;44(2):153–61.

22. Kaplan AR, Glazer PM. Impact of hypoxia on DNA repair and genome integrity. *Mutagenesis*. 2019.

23. Trinkaus ME, Hicks RJ, Young RJ, Peters LJ, Solomon B, Bressel M, et al. Correlation of p16 status, hypoxic imaging using [18F]-misonidazole positron emission tomography and outcome in patients with loco-regionally advanced head and neck cancer. *J Med Imaging Radiat Oncol*. 2014;58(1):89–97.

24. Welz S, Monnich D, Pfannenberg C, Nikolaou K, Reimold M, La Fougere C, et al. Prognostic value of dynamic hypoxia PET in head and neck cancer: results from a planned interim analysis of a randomized phase II hypoxia-image guided dose escalation trial. *Radiother Oncol*. 2017;124(3):526–32.

25. Rohwer N, Zasada C, Kempa S, Cramer T. The growing complexity of HIF-1alpha's role in tumorigenesis: DNA repair and beyond. *Oncogene*. 2013;32(31):3569–76.

26. Wobb J, Krueger SA, Kane JL, Galoforo S, Grills IS, Wilson GD, et al. The effects of pulsed radiation therapy on tumor oxygenation in 2 murine models of head and neck squamous cell carcinoma. *Int J Radiat Oncol Biol Phys*. 2015;92(4):820–8.

27. Calvo-Asensio I, Dillon ET, Lowndes NF, Ceredig R. The transcription factor Hif-1 enhances the radio-resistance of mouse MSCs. *Front Physiol*. 2018;9:439.

28. Liu J, Zhang J, Wang X, Li Y, Chen Y, Li K, et al. HIF-1 and NDRG2 contribute to hypoxia-induced radioresistance of cervical cancer Hela cells. *Exp Cell Res*. 2010;316(12):1985–93.

29. Swartz JE, Pothen AJ, van Kempen PM, Stegeman I, Formsma FK, Cann EM, et al. Poor prognosis in human papillomavirus-positive oropharyngeal squamous cell carcinomas that overexpress hypoxia inducible factor-1alpha. *Head Neck*. 2016;38(9):1338–46.

30. Beasley NJ, Leek R, Alam M, Turley H, Cox GJ, Gatter K, et al. Hypoxia-inducible factors HIF-1alpha and HIF-2alpha in head and neck cancer: relationship to tumor biology and treatment outcome in surgically resected patients. *Cancer Res*. 2002;62(9):2493–7.

31. Winter SC, Shah KA, Han C, Campo L, Turley H, Leek R, et al. The relation between hypoxia-inducible factor (HIF)-1alpha and HIF-2alpha expression with anemia and outcome in surgically treated head and neck cancer. *Cancer*. 2006;107(4):757–66.

32. Norikane T, Yamamoto Y, Maeda Y, Kudomi N, Matsunaga T, Haba R, et al. Correlation of (18)F-fluoromisonidazole PET findings with HIF-1alpha and p53 expressions in head and neck cancer: comparison with (18)F-FDG PET. *Nucl Med Commun*. 2014;35(1):30–5.

33. Sato J, Kitagawa Y, Watanabe S, Asaka T, Ohga N, Hirata K, et al. (18)F-Fluoromisonidazole positron emission tomography (FMISO-PET) may reflect hypoxia and cell proliferation activity in oral squamous cell carcinoma. *Oral Surg Oral Med Oral Pathol Oral Radiol*. 2017;124(3):261–70.

34. Betts GN, Eustace A, Patiar S, Valentine HR, Irlam J, Ramachandran A, et al. Prospective technical validation and assessment of intra-tumour heterogeneity of a low density array hypoxia gene profile in head and neck squamous cell carcinoma. *Eur J Cancer*. 2013;49(1):156–65.

35. Peterle GT, Maia LL, Trivilin LO, de Oliveira MM, Dos Santos JG, Mendes SO, et al. PAI-1, CAIX, and VEGFA expressions as prognosis markers in oral squamous cell carcinoma. *J Oral Pathol Med*. 2018;47(6):566–74.

36. Brockton N, Dort J, Lau H, Hao D, Brar S, Klimowicz A, et al. High stromal carbonic anhydrase IX expression is associated with decreased survival in P16-negative head-and-neck tumors. *Int J Radiat Oncol Biol Phys*. 2011;80(1):249–57.

37. Bittner MI, Wiedenmann N, Bucher S, Hentschel M, Mix M, Rucker G, et al. Analysis of relation between hypoxia PET imaging and tissue-based biomarkers during head and neck radiochemotherapy. *Acta Oncol*. 2016;55(11):1299–304.

38. Schrijvers ML, van der Laan BF, de Bock GH, Pattje WJ, Mastik MF, Menkema L, et al. Overexpression of intrinsic hypoxia markers HIF1alpha and CA-IX predict for local recurrence in stage T1-T2 glottic laryngeal carcinoma treated with radiotherapy. *Int J Radiat Oncol Biol Phys*. 2008;72(1):161–9.

39. Brockton NT, Klimowicz AC, Bose P, Petrillo SK, Konno M, Rudmik L, et al. High stromal carbonic anhydrase IX expression is associated with nodal metastasis and decreased survival in patients with surgically-treated oral cavity squamous cell carcinoma. *Oral Oncol*. 2012;48(7):615–22.

40. Hoogsteen IJ, Marres HA, Wijffels KI, Rijken PF, Peters JP, van den Hoogen FJ, et al. Colocalization of carbonic anhydrase 9 expression and cell proliferation in human head and neck squamous cell carcinoma. *Clin Cancer Res*. 2005;11(1):97–106.

41. Jansen JF, Carlson DL, Lu Y, Stambuk HE, Moreira AL, Singh B, et al. Correlation of a priori DCE-MRI and (1)H-MRS data with molecular markers in neck nodal metastases: initial analysis. *Oral Oncol*. 2012;48(8):717–22.

42. Le QT, Kong C, Lavori PW, O'Byrne K, Erler JT, Huang X, et al. Expression and prognostic significance of a panel of tissue hypoxia markers in head-and-neck squamous cell carcinomas. *Int J Radiat Oncol Biol Phys*. 2007;69(1):167–75.

43. Tsuzuki Y, Fukumura D, Oosthuyse B, Koike C, Carmeliet P, Jain RK. Vascular endothelial growth factor (VEGF) modulation by targeting hypoxia-inducible factor-1alpha–> hypoxia response element–> VEGF cascade differentially regulates vascular response and growth rate in tumors. *Cancer Res*. 2000;60(22):6248–52.

44. Moeller BJ, Cao Y, Li CY, Dewhirst MW. Radiation activates HIF-1 to regulate vascular radiosensitivity in tumors: role of reoxygenation, free radicals, and stress granules. *Cancer Cell*. 2004;5(5):429–41.

45. Pavon MA, Parreno M, Leon X, Sancho FJ, Cespedes MV, Casanova I, et al. Ku70 predicts response and primary tumor recurrence after therapy in locally advanced head and neck cancer. *Int J Cancer*. 2008;123(5):1068–79.

46. Moeller BJ, Yordy JS, Williams MD, Giri U, Raju U, Molkentine DP, et al. DNA repair biomarker profiling of head and neck cancer: Ku80 expression predicts locoregional failure and death following radiotherapy. *Clin Cancer Res*. 2011;17(7):2035–43.

47. Ruhle A, Xia O, Perez RL, Trinh T, Richter W, Sarnowska A, et al. The radiation resistance of human multipotent mesenchymal stromal cells is independent of their tissue of origin. *Int J Radiat Oncol Biol Phys*. 2018;100(5):1259–69.

48. Chan N, Koch CJ, Bristow RG. Tumor hypoxia as a modifier of DNA strand break and cross-link repair. *Curr Mol Med*. 2009;9(4):401–10.

49. Wirthner R, Wrann S, Balamurugan K, Wenger RH, Stiehl DP. Impaired DNA double-strand break repair contributes to chemoresistance in HIF-1 alpha-deficient mouse embryonic fibroblasts. *Carcinogenesis*. 2008;29(12):2306–16.